Anal. Chem. **2007,** *79,* 2463−2471

Molecular Profiling of Native and Matrix-Coated Tissue Slices from Rat Brain by Infrared and Ultraviolet Laser Desorption/Ionization Orthogonal Time-of-Flight Mass Spectrometry

Klaus Dreisewerd,*,† Remi Lemaire,‡ Gottfried Pohlentz,† Michel Salzet,‡ Maxence Wisztorski,‡ Stefan Berkenkamp,§ and Isabelle Fournier‡

Institute of Medical Physics and Biophysics, Westfälische Wilhelms-Universität Münster, Germany, Sequenom GmbH, Hamburg, Germany, and Laboratoire de Neuroimmunologie des Annélides, Université des Sciences et Technologies de Lille, France

Phospho- and glycolipids contained in the plasma membrane of neuronal tissue were profiled by direct infrared laser desorption/ionization orthogonal time-of-flight mass spectrometry (IR-LDI-o-TOF-MS), performed on cryosected native slices generated from rat brain. About 100 different detected lipid species are putatively assigned based on their molecular weight. Spraying of potassium acetate onto the slices was found to facilitate data interpretation in positive ion mode by reducing residual sodium adduct ion intensities. Coating the slices with matrix and using an ultraviolet laser for UV-MALDI-o-TOF-MS extends the analysis to peptides and small proteins but induces analyte diffusion. Peptides and partially cleaved proteins derived from proteolytic digests were recorded after incubation of native sections with trypsin and subsequent coating of the slices with MALDI matrix.

Molecular profiling of biological tissue by matrix-assisted laser desorption ionization mass spectrometry (MALDI-MS) has recently found a wide research interest,[1,2] for example to identify biological markers or for differential analysis studies.[3] In its simplest form MALDI-MS profiling can allow a rapid analysis: simple mixing of a tissue (micro-) section with a suitable matrix can generate a profile of the major peptide/protein content, for example of neuroendocrine tissue,[4] or that of the major phospho- and glycolipid constituents of the cell membranes.[5] More sophisticated matrix preparation protocols allow one to preserve the spatial distribution of analyte molecules within the tissue to a certain extent and to generate a molecular image by scanning the laser across the slices.[6] However, owing to molecular diffusion, the spatial resolution is frequently diminished during the matrix application step. Direct laser desorption ionization (LDI) mass analysis of native slices avoids this critical preparation step and may thus provide a spatial resolution approaching the laser spot diameter. However, lacking the MALDI matrix this approach has in the past essentially been limited to the analysis of small cations or anions within tissue slices and cells.[8,9] Mostly ultraviolet (UV) lasers were used in these studies. Direct infrared (IR-)LDI mass analysis of peptides and small proteins from lyophilized samples[10] or from protein-loaded polyacrylamide gels[11] has been reported in a few studies. In particular, the use of the water of hydration as the "IR matrix" may have its merits for the analysis of tissue cryosections.[10] However, at least for the analysis of peptides and proteins this latter approach seems to be restricted to samples containing exceedingly high concentrations of analyte.[10,11] In contrast to UV-MALDI-MS, where only monolayers of material are desorbed at the ion detection threshold,[12] material on the order of 5−10 μm in thickness is typically ablated by a single IR laser pulse.[13]

The employment of orthogonal (o-)TOF mass spectrometry[14] has been shown to provide substantial advantages if the analysis is to be performed from rough and electrically nonconducting surfaces. MALDI-MS analysis is for example possible with a high mass accuracy directly from high-performance thin-layer chro-

* To whom correspondence should be addressed. E-mail: dreisew@uni-muenster.de.

† Westfälische Wilhelms-Universität Münster.

‡ Université des Sciences et Technologies de Lille.

§ Sequenom GmbH.

(1) Caldwell, R. L.; Caprioli, R. M. *Mol. Cell. Proteomics* **2005**, *4*, 394.
(2) Chaurand, P.; Schwartz, S. A.; Caprioli, R. M. *Anal. Chem.* **2004**, *76*, 87A.
(3) Fournier, I.; Day, R.; Salzet, M. *Neuroendocr. Lett.* **2003**, *24*, 9.
(4) Dreisewerd, K.; Kingston, R.; Geraerts, W. P. M.; Li, K. W. *Int. J. Mass Spectrom.* **1997**, *169*, 291.
(5) Jackson, S. N.; Wang, H. Y. J.; Woods, A. S. *Anal. Chem.* **2005**, *77*, 4523.
(6) Schwartz, S.; Reyzer, M. L.; Caprioli, R. M. *J. Mass Spectrom.* **2003**, *38*, 699.
(7) Spengler, B.; Hubert, M. *J. Am. Soc. Mass Spectrom.* **2002**, *13*, 735.
(8) Proceedings of LAMMA Symposium, Düsseldorf, Germany, October 8−10, 1980, *Fres. Z. Anal. Chem.* **1981**, Vol. *308*.
(9) Hillenkamp, F.; Unsold, E.; Kaufmann, R.; Nitsche, R. *Appl. Phys.* **1975**, *8*, 341.
(10) Berkenkamp, S.; Karas, M.; Hillenkamp, F. *Proc. Natl. Acad. Sci. U.S.A.* **1996**, *93*, 7003.
(11) Rousell, D. J.; Dutta, S. M.; Little, M. W.; Murray, K. K. *J. Mass Spectrom.* **2004**, *39*, 1182.
(12) Dreisewerd, K. *Chem. Rev.* **2003**, *103*, 395.
(13) Menzel, C.; Dreisewerd, K.; Berkenkamp, S.; Hillenkamp, F. *Int. J. Mass Spectrom.* **2001**, *207*, 73−96.
(14) Krutchinsky, A. N.; Loboda, A. V.; Spicer, V. L.; Dworschak, R.; Ens, W.; Standing, K. G. *Rapid Commun. Mass Spectrom.* **1998**, *12*, 508.

10.1021/ac061768q CCC: $37.00
Published on Web 02/17/2007

matography (HPTLC) plates.[15] The decoupling of the desorption/ionization event and the mass analysis is particularly beneficial in combination with IR-MALDI where large amounts of material are ablated per laser pulse. Making use of an effective absorption of the infrared laser energy by tissue components, e.g., by tissue water, IR-MALDI-o-TOF-MS analysis may be performed directly on native samples. In a study performed in parallel to ours, Jackson et al. have recently reported the detection of major phospholipids from native brain tissue, realizing a coupling of direct IR-LDI with a hybrid ion mobility orthogonal extraction TOF mass spectrometer.[16] Mostly sphingomyelin and phosphatidylcholine species were detected in that work.

In the present paper, molecular profiling of cryosected native and matrix-coated rat brain tissue slices by IR-LDI-o-TOF-MS and by UV-/IR-MALDI-o-TOF-MS is reported. Phospho- and glycolipid species are tentatively assigned based on the mass of well-resolved monoisotopic ions. Peptides and small proteins were detected by UV-MALDI-MS after coating of the slices with MALDI matrix. Tryptic digest products were detected after treating native slices with enzyme followed by matrix-coating.

EXPERIMENTAL SECTION

Materials. α-Cyano-4-hydroxycinnamic acid (HCCA), sinapic acid, bradykinin fragment 1−7, substance P, melittin, and potassium acetate were obtained from Sigma-Aldrich (Deisenhoven, Germany) and used without further purification. Trypsin was from Promega (Framingham, MA).

Tissue Preparation. Adult male Wistar rats weighing 250−350 g (animal use accreditation by the French ministry of the agriculture N*o*. 04860) were maintained under standard care. Animals were sacrificed by decapitation and immediately dissected to remove the brain. Frozen sections of either 15 or 60 μm were obtained with a cryotome. Roughly, sections were taken from intereural 12.70, bregma 3.70 to intereural, 1.20 bregma −7.80 of the brain. Slices were thaw-mounted onto standard histology glass slides. Cryosected tissue slices were stored at −20 or −70 °C prior to use.

Tryptic Digest. A total of 30 μL of enzyme solution (33 ng/μL in 25 mM Tris buffer, pH 7.4) were applied onto tissue slices using a micropipette. To reduce solvent evaporation, samples were covered with a small dish. After digestion for either 3 or 10 min at room temperature, the slices were rinsed with 80% ethanol and allowed to dry at room temperature.

Sample Preparation for LDI- and MALDI-MS Analysis. HCCA matrix solution was prepared by dissolving 10−20 mg of HCCA in 1 mL of acetonitrile/0.1% TFA (2:1, v/v). Sinapic acid matrix was prepared by dissolving 20 mg of sinapic acid in 1 mL of acetonitrile/0.1% TFA (1:1, v/v). A volume of matrix solution of 10−20 μL was spread over the tissue sections using a micropipette. The sample was allowed to dry at room temperature, forming a homogeneous microcrystalline preparation. For LDI analysis, samples were thawed under air and condensed water was allowed to evaporate at room temperature. Tissue slices were then either transferred directly into the mass spectrometer or were rewetted with 0.5 M of potassium acetate using a pneumatic nebulizer. Transfer into the mass spectrometer was done after evaporation of solvent.

Orthogonal TOF-Mass Spectrometer. The o-TOF-MS is a modified prototype, similar to the one described by Loboda et al.[17] By default, this instrument is equipped with an N_2 laser emitting 3 ns long pulses at a wavelength of 337 nm and a maximum repetition rate of 30 Hz. The UV laser beam is delivered via a fiber-optical system, producing a spot size on the sample of $\sim 200 \times 230\ \mu m^2$. In our modified version, a second laser port has been added to adopt the beam of an Er:YAG-laser (BiOptics Laser Systeme, Berlin, Germany). This laser emits pulses of ∼100 ns in duration at a wavelength of 2.94 μm and a repetition rate of ∼2 Hz. The IR laser beam irradiates the sample under an angle of incidence of 45°. The focal spot size is approximately $150 \times 200\ \mu m^2$. Samples can be observed with a CCD camera and ∼10 μm resolution. To accommodate glass slides of up to $30 \times 50\ mm^2$ in size and 1.8 mm in thickness, the central part of the sample plate ($50 \times 30\ mm^2$) was milled out to a thickness of ∼2 mm. An adapter was used for 1 mm thick microscopic slides. Substrates were fixed with double sided pads of 0.2 mm thickness.

Ions are generated in an elevated-pressure ion source filled with nitrogen gas ($p \sim 1-5 \times 10^{-1}$ mbar) and are accelerated by a low extraction field of ∼25 V/mm into a quadrupole ion guide. The quadrupole is filled with N_2 at a pressure of $\sim 10^{-3}$ mbar. In normal operation the lower m/z cutoff of the quadrupole was set to m/z 500 in order to optimize ion transmission for the lipid and peptide mass range. To monitor low mass ions, this cutoff was set to m/z 150 in a few experiments. After passing the collisional cooling quadrupole, ions enter the high-vacuum part of the instrument ($p \sim 1 \times 10^{-7}$ mbar) where they are accelerated in orthogonal direction with respect to their original movement. Time-of-flight analysis was performed in both negative (−) and positive (+) ion mode, using acceleration potentials of 10 (−/+) or 20 kV (+) and a repetition rate of the push-out pulser of a few kilohertz. Time-to-digital measurements were typically performed with a bin width of 256 ps. Calibration of the instrument was achieved with a two-point calibration using protonated or deprotonated molecular ions of bradykinin fragment 1−7 and either substance P or melittin desorbed from a regular analyte/matrix preparation. For acquisition of UV-MALDI mass spectra ∼7000 single laser pulses were typically applied according to an acquisition time of ∼4 min at 30 Hz laser repetition rate. Owing to the lower repetition rate of the IR-laser of only 2 Hz and the larger amounts of material ablated per pulse, a maximum of ∼1200 IR-laser pulses was applied for IR-LDI- and IR-MALDI-MS. Laser fluences were adjusted to values moderately above the ion detection threshold for the individual matrix/wavelength combinations. For analysis with the IR laser, the sample plate was typically moved to a neighboring position after a few to ∼ten single exposures whereas for UV-MALDI a few ten to some hundred laser pulses were typically applied on a certain position before the position was changed. Mass spectra were processed using the MoverZ software (vs 2001.02.13, Genomic Solutions, Ann Arbor, MI).

(15) Dreisewerd, K.; Muthing, J.; Rohlfing A.; Meisen I.; Vukelic, Z.; Peter-Katalinic, J.; Hillenkamp, F.; Berkenkamp, S. *Anal. Chem.* **2005**, *77*, 4098.
(16) Woods, A. S.; Ugarov, M.; Jackson, S. N.; Egan, T.; Wang, H. Y. J.; Murray, K. K.; Schultz, J. A. J. *Proteome Res.* **2006**, *5*, 1484.
(17) Loboda, A. V.; Ackloo, S.; Chernushevich, I. V. *Rapid Commun. Mass Spectrom.* **2003**, *17*, 2508.

RESULTS AND DISCUSSION

Direct IR-LDI-MS. Direct IR-LDI-o-TOF mass spectra that were acquired from a cryosected rat brain slice of 60 μm thickness in negative and positive ion mode, respectively, are plotted in Figures 1 and 2. The native slice was sprayed with 0.5 M KAc prior to the MS analysis. The mass spectra were recorded from random positions in a central area of the slice of approximately 5×5 mm^2 in size. In both ion modes, the mass spectra are dominated by a series of ions in the *m/z* range between ~700 and 900 (Figures 1a and 2a). The mass ranges and characteristic mass differences of 2, 16, and 28, observed for several sets of ions (see for example inset in Figure 1a), suggest that these species represent phospholipids with varying fatty acid residues, on the one hand, and glycolipids, in particular hydroxylated and non-hydroxylated sulfatides, on the other. Owing to the high mass resolving power of ~10 000 (fwhm) of the analysis, the identity of these ions may tentatively be assigned based solely on their monoisotopic mass. Major phospho- and glycolipid structures from rat brain tissue have been identified previously in several studies, for example by nanoESI-tandem MS analysis.[18] Likely identities of the detected species are proposed in Tables 1 and 2 for the two ion modes, respectively, along with theoretical *m/z* values and experimentally determined ones using external calibration. The generally good agreement between the values suggests that the detected ion species are indeed likely to represent several of the well-known major phospho- and glycosphingolipids of rat brain plasma membranes: hydroxylated and non-hydroxylated sulfatides (ST, ST-OH), cerebrosides (CB), phosphatidylcholine (PC), phosphatidylethanolamine (PE), phosphatidylglycerol (PG), phosphatidylinositol (PI), plasmenylethanolamine (PlsEtn), phosphatidylserine (PS), and sphingomyelin (SM). Partly, the distributions of lipid species, known to be present in rat brain in high quantity, overlap too closely to allow a differentiation by the mere MS^1 data. For example, the ion at *m/z* 844.51, observed in positive ion mode (Table 2), could equally well represent a ST 38:2 (theoretical *m/z*, 844.50) or a PC 38:6 (844.53) species. Also PA and CB ion species are likely masked by overlapping lipid series. Although variations in the fatty acid chain residues (i.e., the number of C-atoms and the degree of saturation) are straightforwardly detectable, the MS^1 data also do not allow further differentiation as to the site of the modification. For example, the ion at *m/z* 885.54 (Figure 1b) could in principle represent a PI 18:1/16:0 or a PI 18:0/16:1, though the second isoform is naturally occurring in much higher abundance. A differentiation would be possible by tandem MS analysis, for example by using collisional activation. This option was not available on the employed prototype instrument.

The low mass ranges from *m/z* 130−600, recorded in negative and positive ion mode, respectively, are shown in Figures 1b and 2b. The likely identity of some of the detected ions are indicated in the figures. Generally, direct IR-LDI induces only very little fragmentation of the lipids. Only for the most abundant PC's some sizable intensity of PC-N(CH3)$_3$ ion species is observed in positive ion mode next to some lyso-PC's ions of minor abundance (Table 2, Figure 2b). In negative ion mode, alkylates (16:0, *m/z* 255.24; 18:0, *m/z* 283.27; 18:1, *m/z* 281.26) could be assigned (Figure 1b). Further exploration of the identity of low mass ion species was beyond the scope of the present work.

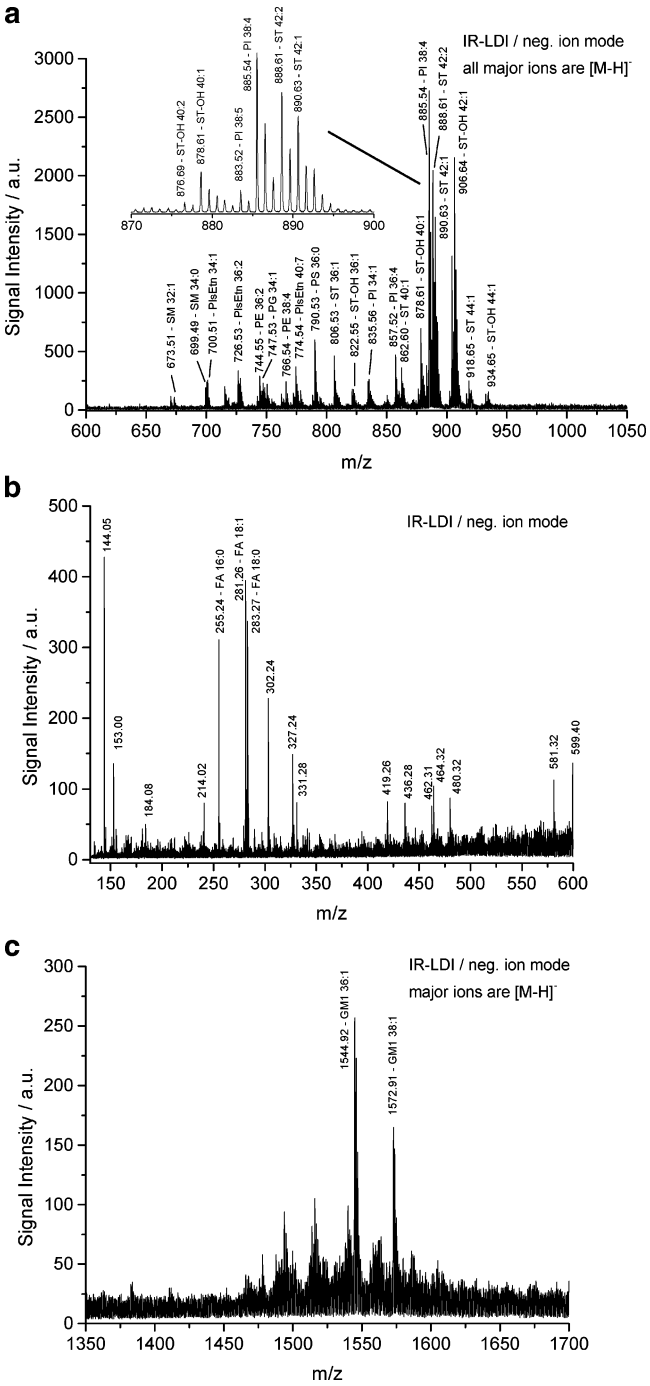

Figure 1. Direct IR-LDI-o-TOF mass spectra recorded from a 60 μm thick rat brain tissue slice in negative ion mode. The tissue slice was sprayed with 0.5 M KAc solution prior to the analysis. (a) *m/z*-range from 600 to 1050, displaying a series of phospholipid and hydroxylated and non-hydroxylated sulfatide species. Major ions are assigned with their putative identity (see Table 1 for an extensive list). All ions represent deprotonated molecular species, $[M - H]^-$. The inset shows an enlarged section displaying the *m/z* range 850 to 900. (b) *m/z* range from 130 to 600; this spectrum was recorded with the low *m/z* cutoff of the quadrupole set to 150. (c) *m/z* range from 1350 to 1700 displaying two putative GM1 ganglioside ions; all other distinct ions presumably represent "unspecific" phospholipid dimers that are produced during the desorption ionization process.

In the negative ion mode, two species that are presumably representing singly sialylated gangliosides, namely GM1 36:1

(18) Lemaire, R.; Wisztorski, M.; Desmons, A.; Tabet, J. C.; Day, R.; Salzet, M.; Fournier, I. *Anal. Chem.* **2006**, *78*, 7145.

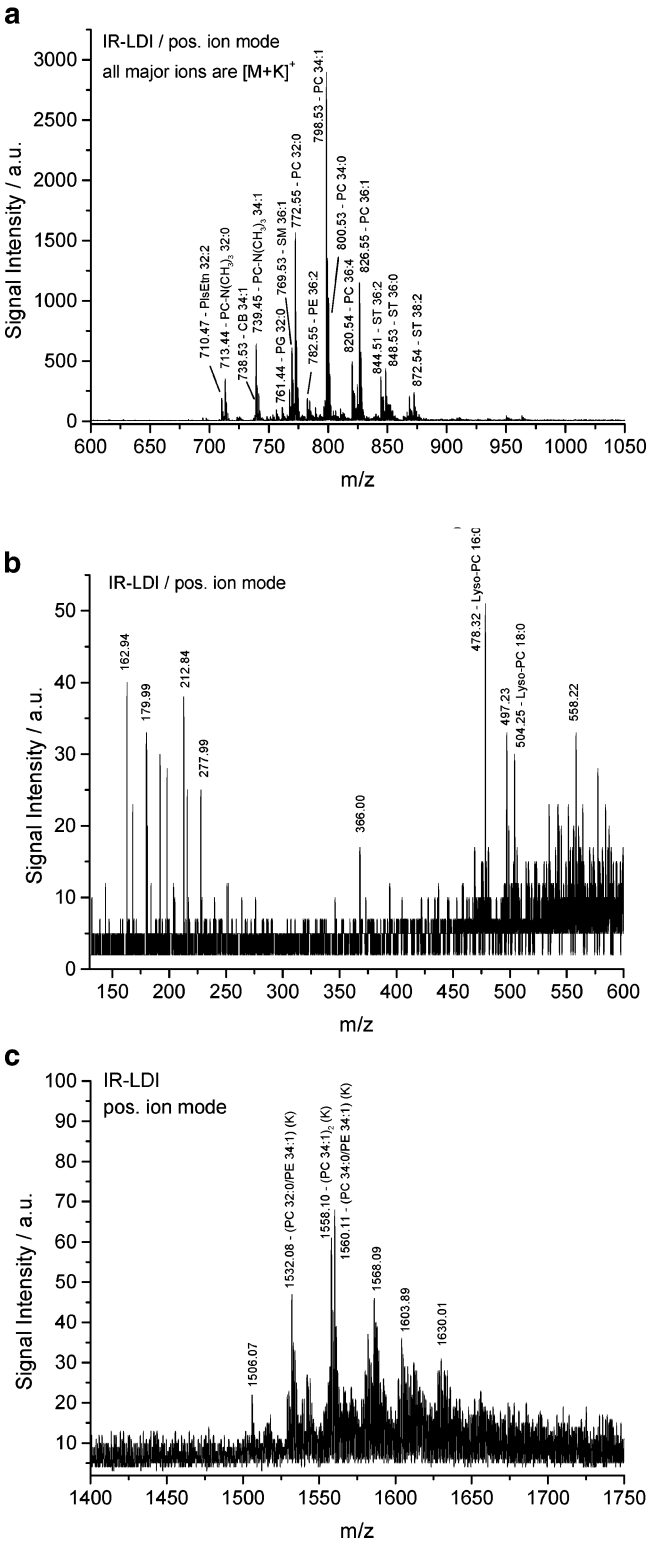

Figure 2. Direct IR-LDI-o-TOF mass spectra recorded from a 60 μm thick rat brain tissue slice in positive ion mode. The tissue slice was sprayed with 0.5 M KAc solution prior to the analysis. (a) *m/z* range from 600 to 1050, displaying a series of phospholipid and sulfatide species. Major ions are assigned with their putative identity (see Table 2 for an extensive list). All major ions represent $[M + K]^+$ ions. (c) *m/z* range from130 to 600; this spectrum was recorded with the low *m/z* cutoff of the quadrupole set to 150. (c) *m/z* range from1400 to 1750. Presumably, only unspecific phospholipid dimers, produced during the desorption ionization process, are detected.

(theoretical *m/z* of the deprotonated molecule, 1544.87) and GM1 38:1 (theoretical *m/z*, 1572.90), are furthermore detected (Figure 1c). Overlap with "unspecific" dimeric ions of smaller phospho- and glycolipids, which are produced within the laser desorption ionization process, renders the identification of possible further ganglioside species difficult. In positive ion mode, distinct ganglioside species could not be differentiated from the background of unspecific gas-phase dimers of smaller lipids (Figure 2c), e.g., $(PC\ 34:1)_2K^+$ at *m/z* 1558.10 (theoretical *m/z*, 1558.09).

Expectedly, more acidic phospholipids are preferentially (or exclusively) detected in the negative ion mode, whereas neutral phospholipids are eventually only detected through cationization with sodium or potassium (e.g., PC). Some phospholipids (e.g., SM, PE) are detected with comparable intensity in both ion modes. Presumably owing to the high natural concentration of potassium in rat brain, even for desorption from native slices positively charged lipids are mainly represented by potassiated molecules $[M + K]^+$ (data not shown). Spraying of the native slices with KAc further reduced residual $[M + Na]^+$ ion intensities and, hence, facilitates data interpretation. Rupture of the cell membranes is not expected to occur as a consequence of the application of KAc solution because intracellular salt concentrations are on the same order of magnitude. Peptide ions of notable intensity do not seem to be produced by direct IR-LDI. Unspecific fragment ions stemming from these and other cell constituents are, however, likely to contribute to the chemical background.

Tables 1 and 2 also provide some information about the relative fatty acid variations within lipid species of a particular type, even if the degree of saturation or varying chain lengths will have a certain influence on proton and cation affinities, and this will, therefore, hamper a more quantitative evaluation. A quantitative comparison of lipids of different type would be even more difficult due to the rather different ionization efficiencies. For a semiquantititave analysis, $^{12}C/^{13}C$, $^{39}K/^{41}K$ isotopic abundances, as well as potential overlap with the distributions of other species need to be further taken into account. Within these limitations, the determined ion abundances suggest, for example, that the ratio of singly unsaturated PC (34:1) to fully saturated PC (34:0) is approximately 2:1−3:1 (Table 2).

Owing to the preservation of the lateral molecular distribution in carefully prepared native slices, the IR-LDI approach seems well suited for imaging MALDI-MS, although the high amount of consumed material will inherently reduce the analytical sensitivity. Previous UV-MALDI-MS studies by Jackson et al.[5] suggest that different phospholipid distributions should be obtained from the cerbellar cortex ("gray matter") versus the cerbellar peduncle ("white matter"). IR-LDI measurements of the two brain areas did as yet not produce really conclusive results, although some differences in lipid distribution are indicated. Compared to the results by Jackson et al. the differences are, however, relatively minor. This finding is eventually owing to the strong averaging by the relative large laser spot size used and positions sampled for the direct LDI mode. We will address this important issue further after completion of a new laser stage, allowing a reduction of focal spot sizes down to ~20 μm in diameter. Owing to non-neglectable analyte diffusion, spatially resolved MALDI measurements were not meaningful with the current crude matrix application protocol.

Table 1. Putative Identities of Phospho- and Glycolipid Species Observed by Direct IR-LDI-o-TOF-MS from Native Rat Brain Tissue Slice in the Negative Ion Mode, Along with the Theoretical and Experimental *m/z* Values of the Monoisotopic Deprotonated Molecular Ion, $[M - H]^-$ [a–c]

expt. *m/z*	theor. *m/z*	identity	signal intensity arb. units	alternatives
599.33	599.32	Lyso-PI 18:0	321	
670.52	670.46	PA 34:2	507	
673.51	673.52	SM 32:1	222	PA 34:1 (673.48)
699.49	699.50	PA 36:2	904	
700.51	**700.53**	**PlsEtn 34:1**	**1019**	
701.51	**701.55**	**SM 34:1**	**1019**	
715.57		?	907	
716.56	716.52	PE 34:1	626	
718.55	718.54	PE 34:0	409	
726.53	**726.54**	**PlsEtn 36:2**	**1430**	
728.56	**728.56**	**PlsEtn 36:1**	**1288**	
742.56	742.54	PE 36:2	487	
744.55	**744.55**	**PE 36:1**	**1274**	
746.54	746.51	PlsEtn 38:7	689	
747.53	747.52	PG 34:1	843	
750.53	750.54	PlsEtn 38:4	934	
754.56	756.58	PlsEtn 38:2	404	
756.59	756.59	PlsEtn 38:1	315	
762.49	762.51	PE 38:6, probably 16:0/22:6[22]	530	PS 34:0 (762.53)
764.51	764.52	PE 38:5	389	
766.54	766.54	PE 38:4	780	
770.56	770.57	PE 38:2	221	
772.56	772.59	PE 38:1	646	
774.55	**774.54**	**PlsEtn 40:7**	**1776**	
776.56	776.56	PlsEtn 40:6	743	
778.57	778.58	PlsEtn 40:5	754	
788.51	788.54	PS 36:1	566	
790.53	**790.56**	**PS 36:0**	**2447**	PE 40:6 (790.54)
792.54	792.55	PE 40:5	660	
794.56	794.57	PE 40:4	470	
806.53	**806.54**	**ST 36:1**	**2078**	
821.54		?	765	
822.55	822.54	ST-OH 36:1	720	
834.56	**834.58**	**ST 38:1**	**1142**	
835.56	**835.53**	**PI 34:1**	**1036**	
850.55	850.57	ST-OH 38:1	354	
857.51	**857.52**	**PI 36:4**	**2162**	
860.58	860.59	ST 40:2	530	
862.61	**862.61**	**ST 40:1**	**1563**	
876.60	876.59	ST-OH 40:2	803	
878.61	**878.60**	**ST-OH 40:1**	**3157**	
883.52	**883.53**	**PI 38:5**	**1508**	
885.54	**885.55**	**PI 38:4**	**13256**	
888.61	**888.62**	**ST 42:2**	**9915**	
890.63	**890.64**	**ST 42:1**	**7943**	
902.62	902.60	ST-OH 42:3	614	
904.62	**904.62**	**ST-OH 42:2**	**6092**	
906.62	**906.63**	**ST-OH 42:1**	**10067**	
908.64	**908.65**	**ST-OH 42:0**	**3173**	
916.67	916.66	ST 44:2	599	
918.65	**918.67**	**ST 44:1**	**997**	
920.64		?	667	
932.64	932.65	ST-OH 44:1	528	
934.65	934.64	ST-OH 44:0	659	
1544.88	**1544.87**	**GM1 36:1**	**1124**	
1572.91	1572.90	GM1 38:1	736	

[a] Slices were sprayed with 0.5 M KAc prior to the analysis. [b] To guide the eye, lipid species detected with high signal intensity (>1000 a.u.) are highlighted. Abbreviations: galactose (Gal); ceramide (Cer); *N*-acetyl neuraminic acid (NeuAc); Galβ1-3GalNAcβ1-4(NeuAcα2-3)Galβ1-4Glcβ-Cer (GM1); phosphatidic acid (PA) phosphatidylethanolamine (PE); phosphatidylglycerol (PG); phosphatidylinositol (PI); phosphatidylserine (PS); plasmenylethanolamine (PlsEtn); sphingomyelin (SM); sulfatide (ST); hydroxylated sulfatide (ST−OH). [c] Note that "signal intensity" is a measure for the peak height at the given *m/z*; possible contributions from overlapping ^{13}C isotopomers of species with lower nominal mass or chemical noise are not corrected for.

IR-MALDI-MS. Abundant lipid ions are also produced by IR-MALDI-MS from HCCA-coated slices (Figure 3a,b). Owing to the higher intensities of sodiated, and the additional generation of protonated ion species, mass spectra acquired in the positive ion mode are more complex. Overall, however, the same lipid species are recorded in positive ion mode IR-MALDI- and by direct IR-LDI-MS. In the negative ion mode, some phospholipids (notably PE, PlsEtn, SM), which are detected in medium to high abundance

Table 2. Putative Identities of Phospho- and Glycolipid Species Observed by Direct IR-LDI-o-TOF-MS from Native Rat Brain Tissue Slice in the Positive Ion Mode, Along with the Theoretical and Experimental *m/z* Values of the Monoisotopic Cationized Ions, $[M + K]^+$ and $[M + Na]^+$ [a–d]

expt. *m/z*	theor. *m/z*	identity	signal intensity arb. units	alternatives
478.32	478.33	Lyso-PC 16:0	129	
504.32	504.35	Lyso-PC 18:0	71	
551.50	551.50	DAG^+ 32:0	78	
577.50	577.52	DAG^+ 34:1	127	
694.50	6494.48	Pls 32:3 (Na)	129	
697.45	697.47	PC-N$(CH3)_3$ 32:0 (Na)	127	
710.47	710.45	PlsEtn 32:2 (K)	879	
713.44	713.45	PC-N$(CH3)_3$ 32:0 (K)	1594	
723.48	723.53	?	160	
725.48	725.55	?	128	
737.44	737.45	PC-N$(CH3)_3$ 34:2 (K)	130	
738.53	738.53	CB 34:1 (K)	235	
739.45	**739.47**	**PC-N(CH3)3 34:1 (K)**	**3155**	
741.46	**741.48**	**PC-N(CH3)3 34:0 (K)**	**1093**	
748.58		?	198	
751.40		?	175	
753.59	753.59	SM 36:1 (Na)	266	
756.53	756.55	PC 32:0 (Na)	462	
761.44	761.47	PG 32:0 (K)	568	
765.47	765.48	PC-N$(CH3)_3$ 36:2 (K)	279	
767.48	**767.50**	**PC-N(CH3)3 36:1 (K)**	**1276**	
769.53	**769.56**	**SM 36:1 (K)**	**2880**	**PC-N(CH3)3 36:0 (K) (769.51)**
770.54	**770.55**	**PlsEtn 36:0 (K)**	**1688**	
772.55	**772.53**	**PC 32:0 (K)**, probably 16:0/16:0[22]	**7195**	
782.54	782.57	PC 34:1 (Na)	928	
784.55	784.58	PC 34:0 (Na)	846	
789.47	789.50	PG 34:0 (K)	571	
793.50	793.51	PC-N$(CH3)_3$ 38:2 (K)	270	
796.51	796.53	PC 34:2 (K)	551	
798.53	**798.54**	**PC 34:1 (K),** probably 16:0/18:1[22]	**14166**	
800.53	**800.56**	**PC 34:0 (K)**	**5018**	
810.57	810.60	PC 36:1 (Na)	504	
812.57	812.61	PC 36:0 (Na)	359	
820.54	**820.53**	**PC 36:4 (K)**	**2302**	
822.51	**822.54**	**PC 36:3 (K)**	**1107**	
824.55	**824.56**	**PC 36:2 (K)**	**1379**	
826.55	**826.57**	**PC 36:1 (K)**	**5671**	
840.43	840.47	ST 36:4 (K)	291	
842.45	842.48	ST 36:3 (K)	214	
844.51	**844.50**	**ST 36:2 (K)**	**1819**	**PC 38:6 (K) (844.53)**
846.52	**846.52**	**ST 36:1 (K)**	**1004**	**PC 38:5 (K) (846.54)**
848.53	**848.56**	**PC 38:4 (K)**	**2190**	
851.61	851.64	SM 42:2 (K)	673	
853.65	853.66	SM 42:1 (K)	394	
854.62	854.60	PC 38:1 (K)	409	
856.48	856.47	ST-OH 36:4 (K)	225	
858.52	858.48	ST-OH 36:3 (K)	109	
863.36		?	192	
866.68		?	196	
868.45	**868.50**	**ST 38:4 (K)**	**1014**	
870.46		ST 38:3(K)	427	
872.54	**872.53**	**ST 38:2 (K)**	**1168**	**PC 40:6 (K) (872.56)**, probably 18:0/22:6[22]
874.55	874.55	ST 38:1 (K)	409	PC 40:5 (K) (874.57)
876.57	876.59	PC 40:4 (K)	274	
878.59	878.60	PC 40:3 (K)	112	
882.64	882.64	PC 40:1 (K)	114	
908.64	908.65	PC 42:2 (K)	80	
910.66	910.67	PC 42:1 (K)	100	

[a] Slices were sprayed with 0.5 M KAc prior to the analysis. [b] The type of cation is denoted in parentheses; protonated lipid species are not detected by IR-LDI, though they are generated by UV- and IR-MALDI. [c] To guide the eye, lipids detected with high signal intensity (>1000 a.u.) are highlighted. Abbreviations: diacylglycerol (DAG); phosphatidylcholine (PC); phosphatidylethanolamine (PE); phosphatidylserine (PS); plasmenylethanolamine (PlsEtn); sphingomyelin (SM); sulfatide (ST); hydroxylated sulfatide (ST-OH). [d] Note that "signal intensity" is a measure for the peak height at the given *m/z*; possible contributions from overlapping ^{13}C isotopomers of species with lower nominal mass, ^{41}K isotopes, or chemical noise are not corrected for.

by IR-LDI (Figure 1b), are apparently suppressed in the IR-MALDI mass spectra (Figure 3a). A similar effect is observed in UV-MALDI-MS analysis (data not shown). This observation comes as a surprise because only part of the tissue (by area below 50%) is visibly covered with HCCA matrix. The suppression may be attributed to extensive gas-phase reactions taking place in the

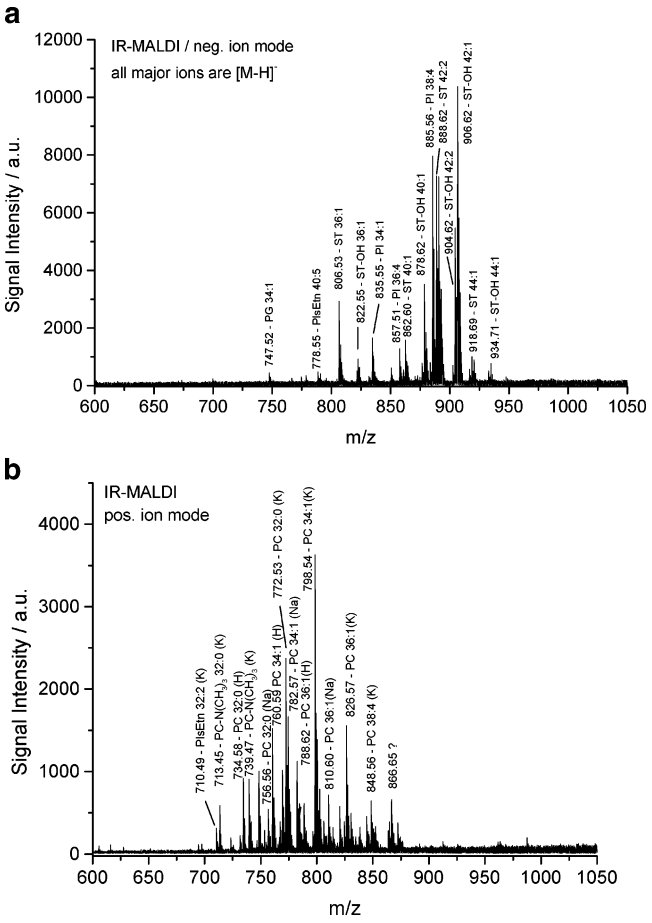

Figure 3. IR-MALDI-o-TOF mass spectrum recorded from a 60 μm thick HCCA-coated rat brain tissue slice in (a) negative and (b) positive ion mode, displaying a series of phospho- and glycolipid species. Some major ions are assigned with their putative identity. In negative ion mode, all ions represent deprotonated molecular species, $[M - H]^-$. In positive ion mode, $[M + H]^+$, $[M + Na]^+$, and $[M + K]^+$ ions are observed with comparable intensities. The type of cation is indicated in parentheses.

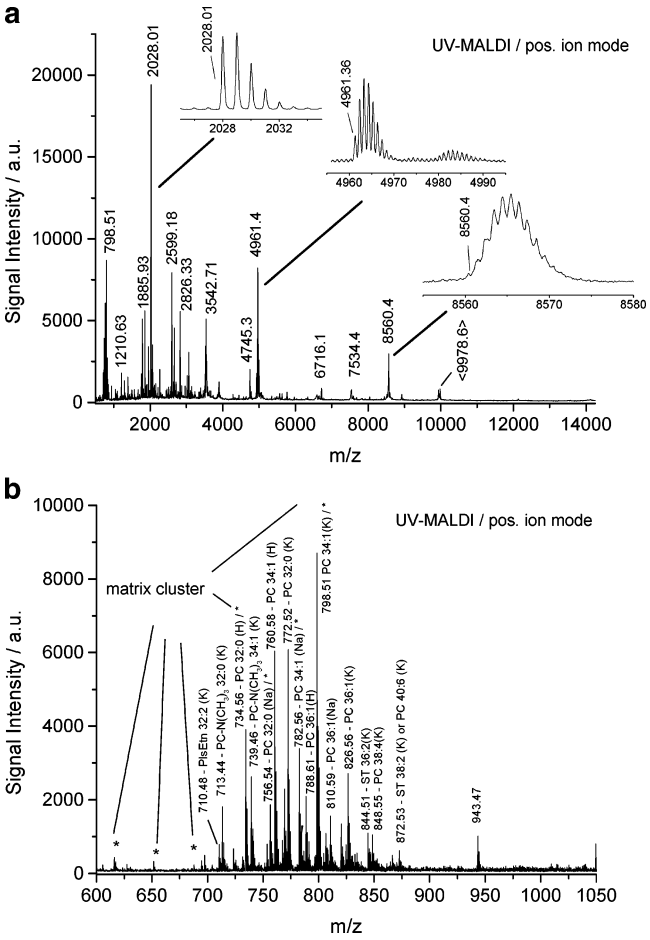

Figure 4. UV-MALDI-o- TOF mass spectrum recorded from a 60 μm thick HCCA-coated rat brain tissue slice in positive ion mode. (a) full mass spectrum (m/z 500−14250). The insets demonstrate the high mass resolution throughout the recorded mass range. m/z values are given for the ^{12}C-monoisotopic peak except for high mass ions for which average molecular weights, denoted by brackets < >, are indicated. (b) m/z range from 600 to 1050, displaying a series of phospho and glycolipid ions. Some major ions are assigned with their putative identity. Ions are observed with comparable intensities as $[M + H]^+$, $[M + Na]^+$, or $[M + K]^+$ ions. Identified matrix cluster ion signals are labeled with an asterisk. "/*" denotes that matrix cluster and lipid ions could not be distinguished. For this experiment, the acceleration potential of the TOF analyzer was set to 20 kV to favor the detection of larger ions.

expanding MALDI plume and thermodynamically favoring certain products. Alternatively, also the use of relatively nonpolar solvent containing 50% acetonitrile, may lead to the observed loss. Further studies are needed to evaluate these effects in more detail. Different matrix systems like 2,5-dihydroxybenzoic acid, which is more commonly used for the analysis of lipids, may also facilitate their detection by MALDI-MS. IR-MALDI-o-TOF-MS analysis of neither HCCA- or sinapic acid coated slices hardly produced any (peptide) ions with molecular weights in excess of 1000. Only some very abundant peptides (as determined by UV-MALDI-MS; see below) also produce some IR-MALDI ions (data not shown). This observation may be attributed to a general lower IR-MALDI ionization efficiency for peptides. Notably—and in some contrast to UV-MALDI-MS measurements (see below)—the degree of matrix cluster formation was found to be rather low if not absent for both IR-MALDI ion polarities.

A substantial drawback accompanying spatially resolved MALDI profiling of tissue is the easy delocalization of molecules from their original lateral position during the matrix preparation step. Indeed, medium intensities of lipids and peptides were well detected from an area just next to the slices to which matrix (and analytes) have eluted during the matrix preparation step (data not shown). Although this problem is clearly aggravated if—like in the current work—rather simple sample preparation protocols are employed, it clearly poses one of the major obstacles for laterally well-resolved MALDI-MS imaging.

UV-MALDI-MS. UV-MALDI-o-TOF-MS analysis of HCCA-coated slices extends the detectable mass range to about 10 000 Da. Figure 4a displays an UV-MALDI-o-TOF mass spectrum that was recorded from an HCCA-coated slice in positive ion mode. The use of sinapic acid extended the accessible mass range even further—to about an m/z of 40 000 (data not shown). The negative ion mode produced only comparatively low ion abundances for both matrices (data not shown). Ions above 1000 Da are in their majority believed to represent peptides and small proteins.[2] As demonstrated by the insets in Figures 4a, up to about an m/z of ~9000 ^{12}C-isotopic resolution is achieved by the o-TOF-analysis. In comparison to typical axial-UV-MALDI-TOF measurements

from tissue slices,[19] this constitutes a substantial improvement. An experiment, in which neighboring slices have been analyzed in parallel by axial- and o-TOF-MS, showed that essentially the same peptides are, however, detected by both methods (data not shown). Further going peptide identification was beyond the scope of the present study

High abundances of phospholipid and sulfatide ions are also generated by positive ion mode UV-MALDI (Figure 4b), by pattern essentially identical to those recorded in the IR-MALDI-MS analysis (Figure 3a). Alike for peptides, lipid ion abundances are substantially lower in negative ion mode mass spectra (data not shown). The potential overlap with smaller peptides (e.g., the ion observed at m/z 943.47 in Figure 4b probably presents such a peptide) and matrix cluster ions complicate the data interpretation. A few matrix cluster ions are assigned in Figure 4b with an asterisk—these species were identified from a mass spectrum that was taken from a pure matrix sample. The degree of matrix cluster formation is notably higher for UV- than for IR-MALDI. Adduct complexes between analyte (both lipid and peptide) and matrix can form another concern, in particular if cinnamic acid derivatives are employed as matrix.[20,21] The extent of adduct formation seems to depend critically on the exact sample preparation conditions—such complexes were in fact observed in a minority of the performed experiments. Comparing standard microcrystalline peptide/matrix MALDI preparations and the preparations on lipid rich tissue, the degree of both matrix cluster and adduct complex formation was generally found to be (much) lower for the tissue preparations or even essentially absent.

UV-MALDI-MS Analysis of Tissue Treated with Trypsin. Molecular identification based on the mass of the detected ion alone is rarely unequivocal. Immunology may provide specific identification but is restricted to individual target structures.[22] MALDI tandem-MS may be used for structural analysis and identification of small molecules directly from tissue sections but would typically be limited to ions not exceeding 2000−3000 Da in mass. Enzymatic digestion of peptidergic components contained—and being accessible to the enzyme—in the tissue may form an interesting "shotgun" approach to cleave larger peptides and proteins to product ion sizes falling well into this mass range.[23] Large proteins that are not detectable by direct MALDI-MS of the original tissue sample may even become demasked. Owing to the high number of enzymatic fragment ions which will in general be produced by this approach, a high resolving power of the mass spectrometer for differentiation of precursor ion species will be compulsory.

Figure 5 demonstrates the principle feasibility of this approach. In this experiment, trypsin was applied for 3 min before the slice was rinsed with ethanol and HCCA matrix was added. In addition to smaller tryptic peptides in the typical mass range, this approach produces a set of larger (and new) ions with m/z values up to above ~25 000. Presumably, these species represent partially cleaved larger proteins that do not show up in the mass spectrum taken from the untreated sample. Autolysis ions of trypsin could not be identified. The exceedingly large number of ion signals in the tryptic fragment mass range renders a data bank search less meaningful, but the results clearly demonstrate that tandem-MS analysis on such a preparation should be possible. Applying trypsin for longer times leads to more complete digestion but also more complex mass spectra (data not shown); this may help to produce fragment ion sizes amenable for tandem MS analysis.

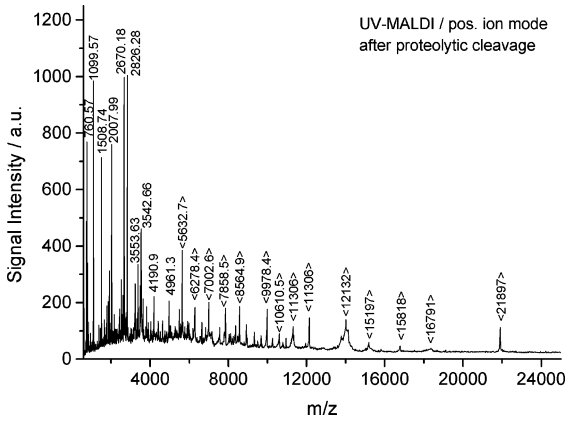

Figure 5. UV-MALDI-o- TOF mass spectrum recorded in positive ion mode from a 15 μm thick rat brain tissue slice, after allowing enzymatic digestion with trypsin directly on the slice for 3 min (at room temperature). The digestion reaction was stopped by rinsing the slices with 80% ethanol and subsequent application of HCCA matrix.

CONCLUSIONS

Molecular analysis of tissue slices employing a MALDI ion source operated at an elevated pressure of ~1 mbar and combined with an orthogonal TOF mass analyzer provides several advantageous features. The analysis can be performed with slices of almost arbitrary thickness without degradation of a high and mass-independent resolving power of about 10 000. For convenience and compatibility with histology, tissue slices can also be prepared on standard glass substrates. The employment of an IR-laser allows to generate spatially resolved phospho- and glycolipid profiles even from native cryosected slices. Spraying of a concentrated KAc solution onto the slices was found to facilitate data interpretation in positive ion mode by effectively reducing the formation of sodium-adduct ions. An important feature of the direct LDI approach is that analyte diffusion is essentially avoided and data recorded as a function of lateral position thus reflect a "true" image of the lipid distribution, at least on a micrometer scale. We will address this issue of achievable lateral resolution further in succeeding work employing smaller laser sizes. In contrast to UV- or IR-MALDI-MS, matrix-less IR-LDI produces no protonated lipids, suggesting additional ionization pathways being effective in the MALDI-case. UV-MALDI-o-TOF-MS allows the profiling of peptides and small proteins from matrix-coated tissue. Larger proteins can partially be demasked by treatment of the tissue with trypsin. Employing miniaturized digestion and matrix preparation protocols in combination with structural analysis and protein identification by tandem MS may therefore allow spatially resolved shot-gun proteomics directly from tissue slices.

ACKNOWLEDGMENT

The authors are grateful to Sequenom GmbH (Hamburg, Germany) for use of their o-TOF instrument. We also thank Franz

(19) Lemaire, R.; Tabet, J. C.; Ducoroy, P.; Hendra, J. B.; Salzet, M.; Fournier, I. *Anal. Chem.* **2006**, *78*, 809.
(20) Ivleva, V. B.; Elkin, Y. N.; Budnik, B. A.; Moyer, S. C.; O'Connor, P. B.; Costello, C. E. *Anal. Chem.* **2004**, *76*, 6484.
(21) Krutchinsky, A. N.; Chait, B. T. *J. Am. Soc. Mass Spectrom.* **2002**, *13* 129.
(22) Salzet, M.; Wattez, C.; Slomianny, M. C. *Comp. Biochem. Physiol. Comp. Physiol.* **1993**, *104*, 75.
(23) Chaurand, P.; Stoeckli, M.; Caprioli, R. M. *Anal. Chem.* **1999**, *71*, 5263.

Hillenkamp for support of the project, and Andreas Rohlfing and Sarah Kruppe for technical assistance. This work was supported by grants from Centre National de la Recherche Scientifique (CNRS), Ministère de la Recherche et des Technologies (MRT, ACI jeunes Chercheurs to I.F.), Foundation pour la Recherche Médicale (FRM, to I.F.), Génopole-Lille to M.S. Financial support by the Deutsche Forschungsgemeinschaft (Grant DR 416/5-1) is furthermore acknowledged.

Received for review September 19, 2006. Accepted December 28, 2006.

AC061768Q